

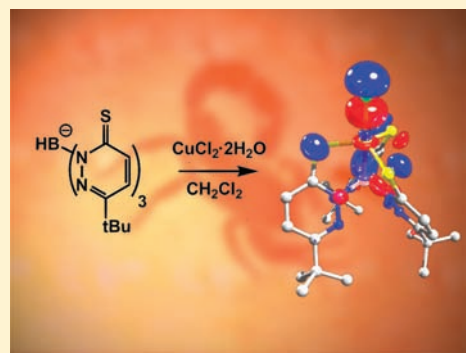
Pyridazine Based Scorpionate Ligand in a Copper Boratrane Compound

Gernot Nuss,[†] Gerald Saischek,[†] Bastian N. Harum,[†] Manuel Volpe,[†] Ferdinand Belaj,[†] and Nadia C. Möscher-Zanetti^{*,†}

[†]Institut für Chemie, Karl-Franzens-Universität Graz, Schubertstrasse 1, A-8010 Graz, Austria

Supporting Information

ABSTRACT: Reaction of potassium tris(mercapto-*tert*-butylpyridazinyl)borate $K[Tn^{tBu}]$ with copper(II) chloride in dichloromethane at room temperature led to the diamagnetic copper boratrane compound $[Cu\{B(Pn^{tBu})_3\}Cl]$ (Pn = pyridazine-3-thionyl) (**1**) under activation of the B–H bond and formation of a Cu–B dative bond. In contrast to this, stirring of the same ligand with copper(I) chloride in tetrahydrofuran (THF) gave the dimeric compound $[Cu\{Tn^{tBu}\}]_2$ (**2**) where one copper atom is coordinated by two sulfur atoms and one hydrogen atom of one ligand and one sulfur of the other ligand. Hereby, no activation of the B–H bond occurred but a 3-center-2-electron B–H...Cu bond is formed. The reaction of copper(II) chloride with $K[Tn^{tBu}]$ in water gave the same product **2**, but a formal reduction of the metal center from Cu(II) to Cu(I) occurred. When adding tricyclohexyl phosphine to the reaction mixture of $K[Tn^R]$ (R = *t*Bu, Me) and copper(I) chloride in MeOH, the distorted tetrahedral Cu complexes $[Cu\{Tn^R\}(PCy_3)]$ (R = *t*Bu **3**, Me **4**) were formed. Compound **4** is exhibiting an “inverted” κ^3 -H,S,S coordination mode. The copper boratrane **1** was further investigated by density functional theory (DFT) calculations for a better understanding of the M→B interaction involving the d^8 electron configuration of Cu.



INTRODUCTION

Scorpionate ligands have become very popular in the field of coordination chemistry, catalysis, and biomimetic chemistry¹ since the discovery of tris(pyrazolyl)borate (Tp, Figure 1) by

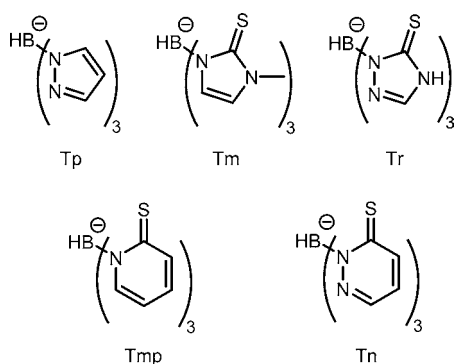


Figure 1. Variation in tripodal scorpionate ligands.

Trofimenko in the mid 1960s.² Their popularity is owed to the variability of the substituents on the pyrazole ring which affect both steric and electronic properties of the ligand. Pyrazolylborates are tridentate ligands where the three nitrogen atoms of the pyrazole are coordinating to the metal giving a soft donor. A further development in scorpionate chemistry was the invention of tris(mercaptoimidazolyl)borate ligands (Tm)³ and later tris(thioxotriazolyl)borate (Tr),⁴ tris(mercaptoimidazolyl)borate

(Tmp)⁵ and recently tris(mercaptoimidazolyl)borate (Tn)⁶ which are considered to be even softer analogues of poly(pyrazolyl)borates (Figure 1). However, limitations of this analogy were observed, and they can be explained by the lower ring strain caused by the larger chelate ring in Tm compared to Tp ligands. Also, the coordinating sulfur in Tm ligands causes large differences in coordination behavior and in reactivity of the respective complexes compared to the coordinating nitrogen in Tp containing complexes. This is because sulfur atoms have lone pairs which can add π -basic character to the metal–ligand bond therefore causing the Tm ligand to be more basic compared to Tp.⁷ Another important impact of sulfur lone pairs on the properties of the Tm ligand is the weak field character compared to Tp ligands.⁷ Hence, $[Fe(Tm^Me)_2]$ ⁸ is a paramagnetic d^6 high spin compound compared to $[Fe(Tp^Me)_2]$,⁹ which shows an interesting spin cross over behavior. These sulfur containing scorpionate ligands can coordinate to the metal in a monodentate (κ^1 -S), bidentate (κ^2 -S,S or κ^2 -H,S), and tridentate (κ^3 -S,S,S or κ^3 -H,S,S) fashion although the κ^3 -S,S,S coordination mode is the most common for Tm^R ligands.⁷ In spite of the soft nature of these ligands, coordination is not only restricted to soft mid to late transition metals in low oxidation states^{8,10} but also coordination to harder early transition metals in high oxidation states (Nb^V, Ta^{III–V}, Ti^{III–IV}, Zr^{IV})¹¹ is observed despite the mismatch in the “soft acid/soft

Received: August 2, 2011

Published: November 17, 2011



base" concept. One of the initial goals to synthesize these ligands was the mimicking of sulfur rich active sites of metallo-enzymes and especially copper containing active sites⁷ as found in cytochrome c oxidase,¹⁰ nitrite reductase,¹³ and metallothionein.¹⁴ The first attempts to model complexes with Tm were hindered by oxidative degradation of the ligand, which demonstrated the sensitivity toward metal ions such as Cu(II) and Fe(III).⁷ The phenomenon of oxidative ligand cleavage of sulfur scorpionates under concurrent reduction of the metal ion was also observed by our group employing the Tn moiety with first-row transition metal salts such as Co(II) and Ni(II).⁶ Nevertheless, there are numerous complexes known containing the Tm moiety, with copper(I) coordinating in a monomeric $[\text{Cu}\{\text{Tm}\}]^3$ or dimeric $[\text{Cu}\{\text{Tm}^{\text{xylyl}}\}]_2$ ¹¹ fashion, whereas when phosphines are added to the reaction, only monomeric $\kappa^3\text{-S,S,S}$ and $\kappa^3\text{-H,S,S}$ coordinated phosphine complexes are observed.¹²

In certain cases boratrane complexes are formed, exhibiting an interesting $\text{M}\rightarrow\text{B}$ dative bond.

The thereby formed hydride leads to reduction of the involved metal ion. Such boratrane complexes containing the Tm moiety are known with Fe, Ru, Os, Co, Rh, Ir, Ni, Pd, and Pt as the coordinating metal,¹³ but there is no evidence of a Cu boratrane containing a tripodal soft $\kappa^3\text{-S,S,S}$ ligand. Although there are few complexes known containing a $\text{Cu}\rightarrow\text{B}$ dative bond,¹⁴ the only known Cu boratrane is Bourissou's $[\text{Cu}\{\text{B}(\text{C}_6\text{H}_4\text{P}(\text{iPr})_2)_3\}\text{Cl}]$.¹⁵

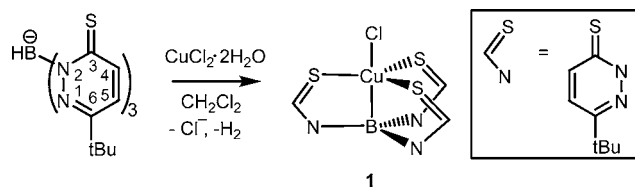
Recently, we reported the synthesis of a series of novel soft tridentate ligands $\text{K}[\text{Tn}^{\text{R}}]$ ($\text{R} = \text{tBu}, \text{Me}, \text{Ph}$) and their coordinational behavior toward Co(II) and Ni(II) centers.⁶ Interestingly, boratrane compounds were formed, both, in CH_2Cl_2 and water. Simultaneous activation of the B–H bond occurred, resulting in a $\text{M}\rightarrow\text{B}$ dative bond and a $\kappa^4\text{-B,S,S,S}$ coordination mode of the $\text{B}(\text{Pn}^{\text{tBu}})_3$ ($\text{Pn}^{\text{tBu}} = 6\text{-tert-butylpyridazine-3-thione}$) moiety.

Here, we report the reactivity of the tris(pyridazinethionyl)-borate ligand toward copper(II) and copper(I) salts thereby presenting the first copper boratrane compound bearing a sulfur rich environment.

RESULTS AND DISCUSSION

Synthesis of the Compounds. The reaction of the scorpionate ligand $\text{K}[\text{Tn}^{\text{tBu}}]$ ⁶ with copper(II) chloride in dichloromethane at room temperature led to the diamagnetic boratrane compound $[\text{Cu}\{\text{B}(\text{Pn}^{\text{tBu}})_3\}\text{Cl}]$ (**1**) in moderate yield (Scheme 1). The orange product precipitates after one day of stirring. After filtration, the crude orange product was washed

Scheme 1. Formation of Boratrane Compound $[\text{Cu}\{\text{B}(\text{Pn}^{\text{tBu}})_3\}\text{Cl}]$ (**1**) and Numbering Scheme



with water, MeOH, and diethyl ether to purify it from byproducts. Recrystallization from a CH_2Cl_2 solution gave red crystals suitable for X-ray diffraction analysis. Proton and carbon NMR spectra of **1** in $\text{DMSO-}d_6$ show sharp resonances in the expected regions for the atoms of the symmetrically

coordinated scorpionate ligand confirming the formation of a diamagnetic copper compound.

Similar to our earlier observations in cobalt and nickel complexes with the same ligand, no absorption for a B–H stretch frequency could be observed by IR spectroscopy. This is in contrast to related scorpionate ligands containing the tris(mercaptoimidazolyl)borate moiety, where B–H frequencies appear as distinctive frequencies around 2400 cm^{-1} , and significant shifts are observed when the ligands are coordinated to a metal.²⁰ The formation of a boratrane compound was clearly evidenced by the determination of its molecular structure by single crystal X-ray diffraction analysis, where the short Cu–B distance of $2.060(3)\text{ \AA}$ leaves no space for hydrogen. A molecular view of compound **1** is shown in Figure 2, selected bond lengths and angles are given in Table 1, and

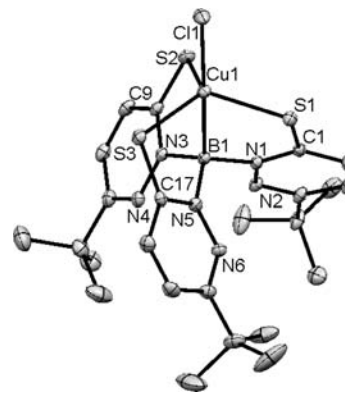


Figure 2. Molecular structure of $[\text{Cu}\{\text{B}(\text{Pn}^{\text{tBu}})_3\}\text{Cl}]$ (**1**) with thermal ellipsoids at 45% probability.

Table 1. Selected Bond Lengths (Å) and Angles (deg) of **1**

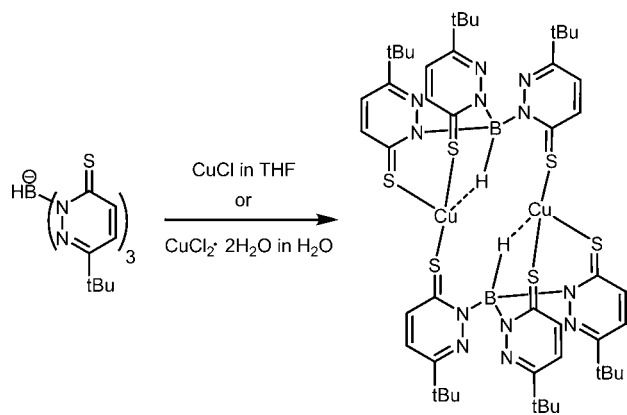
Cu1–B1	2.060(3)	S1–Cu1–S2	115.35(3)
Cu1–S1	2.3544(9)	S2–Cu1–S3	118.60(3)
Cu1–S2	2.3204(9)	S1–Cu1–S3	117.31(3)
Cu1–S3	2.3156(9)	S1–Cu1–B1	80.03(9)
Cu1–Cl1	2.2821(9)	S2–Cu1–B1	80.06(9)
S1–C1	1.710(3)	S3–Cu1–B1	80.11(9)
S2–C9	1.706(3)	S1–Cu1–Cl1	101.53(3)
S3–C17	1.704(3)	S2–Cu1–Cl1	98.99(4)
B1–N1	1.537(4)	S3–Cu1–Cl1	99.30(3)
B1–N3	1.528(4)	B1–Cu1–Cl1	178.42(9)
B1–N5	1.530(4)	S1–Cu1–S2	115.35(3)

crystallographic data is given in Table 6. Copper boratrane complexes are extremely rare and have not been reported with related sulfur based scorpionate ligands. The Cu–B bond found in **1** (Cu1–B1 $2.060(3)\text{ \AA}$) is significantly shorter compared with that in the only other known copper boratrane complex $[\text{Cu}\{\text{B}(\text{C}_6\text{H}_4\text{P}(\text{iPr})_2)_3\}\text{Cl}]$ ($2.508(2)\text{ \AA}$).¹⁵ The electrophilic nature of the pyridazine heterocycle leads to a more electrophilic boron which possibly shortens the boron copper bond. However, the distance is comparable to those found in analogous pyridazine bearing boratranes synthesized by our group recently, exhibiting $2.016(3)$ and $2.068(3)\text{ \AA}$ for $[\text{Ni}\{\text{B}(\text{Pn}^{\text{tBu}})_3\}\text{Cl}]$ and $[\text{Co}\{\text{B}(\text{Pn}^{\text{tBu}})_3\}\text{Cl}]$, respectively.⁶ The geometry at copper in **1** can best be described as distorted trigonal bipyramidal, exhibiting an almost perfectly linear B1–Cu1–Cl1 bond angle of $178.42(9)^\circ$. The S–Cu–S angles varying between $115.35(3)$ and $118.60(3)^\circ$ show significant

deviation from the ideal angle. The three pyridazines are paddlewheel like twisted around the copper therefore causing the sulfur copper chlorine angles to range between 98.99(4) and 101.53(3)° which is comparable to the phosphine copper chlorine angles of Bourissou's first Cu boratrane (99.79(2)°).

Treatment of a solution of $K[Tn^{tBu}]$ with CuCl in THF gave a copper(I) compound, namely, $[Cu\{Tn^{tBu}\}]_2$ (**2**), but in contrast to **1** the ligand remains an anionic scorpionate (Scheme 2). The product was isolated as a red product in good yield, and crystals suitable for X-ray diffraction analysis were obtained by

Scheme 2. Formation of $[Cu\{Tn^{tBu}\}]_2$ (**2**)



crystallization from a dichloromethane solution. A molecular view of **2** is given in Figure 3. Selected bond lengths and angles are shown in Table 2 and crystallographic data are given in Table 6.

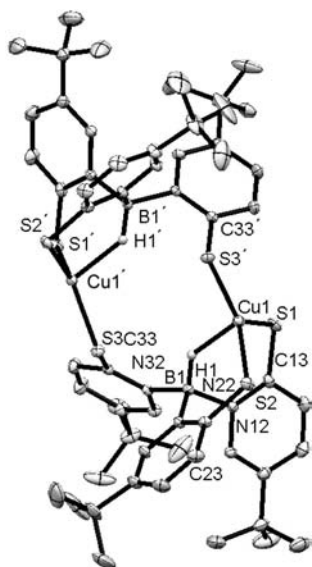


Figure 3. Molecular structure of $[Cu\{Tn^{tBu}\}]_2$ (**2**) with thermal ellipsoids at 45% probability.

The structure analysis revealed a species consisting of two $[Cu\{Tn^{tBu}\}]$ units which coordinate to the copper ion via two sulfur atoms and the hydride (Scheme 2). The third sulfur atom of the ligand forms a bridge to the second unit of $[Cu\{Tn^{tBu}\}]$ leading to a tetra-coordinate copper ion with a S_3H coordination sphere of a (3 + 1) type. The boron center exhibits an “ S_3 -inverted” conformation mode, allowing a 3-center-2-electron B–H...Cu bond. The geometry of the dimeric compound can

Table 2. Selected Bond Lengths (Å) and Angles (deg) of $[Cu\{Tn^{tBu}\}]_2$ (**2**)

Cu1–Cu1'	5.0728(3)	S1–Cu1–S2	114.76(1)
Cu1–H1	1.92(2)	S2–Cu1–S3'	120.45(1)
Cu1–B1	2.798(1)	S1–Cu1–S3'	123.96(1)
Cu1–S1	2.2720(4)	H1–Cu1–S1	84.4(1)
Cu1–S2	2.2939(4)	H1–Cu1–S2	85.7(6)
Cu1–S3'	2.2235(4)	H1–Cu1–S3'	107.9(6)
S1–C13	1.707(1)	Cu1–S1–C13	99.91(5)
S2–C23	1.706(2)	Cu1–S2–C23	110.95(5)
S3–C33	1.715(1)	Cu1–S3'–C33'	106.69(5)
B1–N12	1.563(2)	N12–B1–N22	106.3(1)
B1–N22	1.554(2)	N12–B1–N32	110.8(1)
B1–N32	1.556(2)	N22–B1–N32	109.8(1)

be explained by the high flexibility of Tn^{tBu} , which can cause the Pn^{tBu} moiety to rotate around the B–N bond to better accommodate the two copper atoms. This flexibility and behavior toward copper is already known with similar Tm and Tr ligands.^{15,20} The compound is diamagnetic as expected for Cu(I) which is ruling out the formation of a copper(II) species. Thus, based on the solid state structure (Figure 3), in the 1H NMR spectrum of **2** two sets of resonances for Pn^{tBu} substituents in 2:1 ratio are expected. However, the room temperature 1H NMR spectrum shows resonances for only one type of pyridazine ring. Low temperature NMR down to -40 °C did not resolve the resonances of the unsymmetric compound **2** indicating a dynamic behavior in solution. In contrast to this, the unsymmetric aromatic moiety could be distinguished in the low temperature 1H NMR spectra for $[Cu\{Tp^{tBu}\}]_2$ ¹⁶ and $[Cu\{Tr^{Me,o-Py}\}]_2$.¹⁷ Interestingly, the hydride is missing in the 1H NMR spectrum. This phenomenon can be observed for similar complexes containing sulfur scorpionates where the hydride is pointing toward the metal.^{11,18} ^{11}B NMR spectra showed no resonances, similar to other Tn containing complexes.⁶

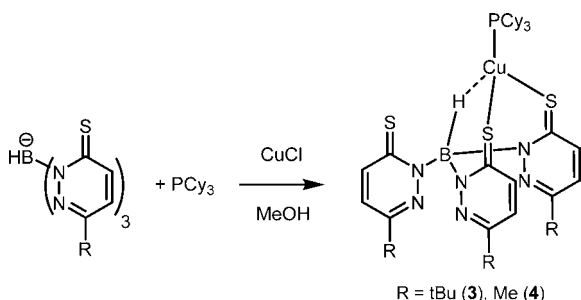
The copper sulfur distances are 2.2720(4) for Cu1–S1, 2.2939(4) for Cu1–S2, and 2.2235(4) for Cu1–S3', which is in the range of related compounds in the literature.^{11,17,18} The geometry at copper of the dimeric compound **2** is best described as distorted trigonal toward the tetrahedral one. The sulfur copper sulfur angles are deviating significantly, ranging from 114.76(1) to 123.96(1)° for S1–Cu1–S2 and S1–Cu1–S3', respectively. This distortion can also be found in related dimeric copper compounds in the literature, where the copper center is surrounded by three sulfurs in an almost trigonal fashion exhibiting sulfur copper sulfur angles between 105.20(4) and 134.98(4)° for $[Cu\{Tr^{Et,Me}\}]_2$ ¹⁸ and between 111.54(4) and 124.64(4)° for $[Cu\{Tr^{Me,o-Py}\}]_2$.¹⁷ The deviation from the ideal trigonal geometry toward the tetrahedral one can be explained by the 3-center-2-electron B–H...Cu interaction, which is evidenced by a H–Cu distance of 1.92(2) Å. This is significantly shorter compared to the H–Cu distance found in $[Cu\{Tr^{Et,Me}\}]_2$ (2.29(3) Å) whereas it is more similar to $[Cu\{Tr^{Me,o-Py}\}]_2$ (1.94(4) Å)¹⁸ and $[Cu\{Tr^{Mes,Me}\}]_2$ (1.99(3) Å).¹⁷ The hydrogen copper bond is almost perpendicular to the CuS_3 plane, which is confirmed by the hydrogen copper sulfur angles of 84.4(1)° for H1–Cu1–S1 and 107.9(6)° for H1–Cu1–S3'. The nitrogen boron nitrogen bonds vary between 106.3(1) and 110.8(1)° for N12–B1–N22 and N12–B1–N32, respectively, exhibiting a distorted tetrahedral geometry at the boron. The distance between the two copper centers in $[Cu\{Tn^{tBu}\}]_2$ is 5.0728(3) Å, which is too large for a possible Cu–Cu interaction.

This distance is longer compared to $[\text{Cu}\{\text{Tr}^{\text{Et,Me}}\}]_2$ (av. 4.2569 (6) Å) and shorter compared to $[\text{Cu}\{\text{Tr}^{\text{Mes,Me}}\}]_2$ (5.401(1) Å) and $[\text{Cu}\{\text{Tr}^{\text{Me,o-Py}}\}]_2$ (5.308(1) Å).

Compound **2** was also obtained via an alternative method using $\text{CuCl}_2 \cdot 2\text{H}_2\text{O}$ in water where product formation was indicated as a red precipitate. Reduction of the metal to copper(I) under decomposition of the scorpionate ligand with formation of the disulfide ($\text{Pn}^{\text{tBu}}\text{-Pn}^{\text{tBu}}$) from Pn^{tBu} occurred, as evidenced by ESI-MS, which shows a mass peak at 335 for $[\text{Pn}^{\text{tBu}}\text{-Pn}^{\text{tBu}} + \text{H}]^+$. For this reason the yield of **2** prepared by method 2 is significantly lower when compared to method 1. This conforms with examples in the literature, where thiols were oxidized to disulfides by metal ions as, for example, Cu^{2+} , Ni^{2+} , or Co^{2+} under concurrent reduction of the metal.^{3,6} The crystal structure of $[\text{Ni}\{\text{B}(\text{Pn}^{\text{Me}})_3\}\text{Cl}]$ was even showing the disulfide $\text{Pn}^{\text{Me}}\text{-Pn}^{\text{Me}}$, which was formed as a byproduct.⁶

The formation of the dimer **2** prompted us to explore the reaction with additional donors. We expected phosphines to be better ligands than the thione sulfur atom. Thus, a solution of $\text{K}[\text{Tn}^{\text{tBu}}]$ and tricyclohexyl phosphine in methanol was treated with CuCl (Scheme 3). Compound $[\text{Cu}\{\text{Tn}^{\text{tBu}}\}(\text{PCy}_3)]$ (**3**) precipitated from the reaction mixture as red material and was

Scheme 3. Preparation of the Phosphine Compounds $[\text{Cu}\{\text{Tn}^{\text{R}}\}(\text{PCy}_3)]$ (R = tBu **3**, Me **4**)



obtained in good yield after workup. The analogous compound $[\text{Cu}\{\text{Tn}^{\text{Me}}\}(\text{PCy}_3)]$ (**4**) was obtained by employing the methyl derivative $\text{K}[\text{Tn}^{\text{Me}}]$, PCy_3 , and CuCl in methanol. The latter was crystallized from a dichloromethane solution, giving orange crystals which were suitable for X-ray diffraction analysis that revealed a similar bonding situation of the scorpionate ligand as in compound **2**. Again, a $\kappa^3\text{-H,S,S}$ coordination mode is observed but the sulfur atom of a second ligand is replaced by the phosphine. Thus, in the respective ^1H NMR spectra of **3** and **4** two sets of resonances for the pyridazine moieties are expected. However, similar to **2**, only one set of pyridazine resonances are observed at room temperature, which is an analogical behavior compared to Dyson's compound $[\text{Cu}\{\text{H}_2\text{B}(\text{mp})_2\}(\text{PCy}_3)]$ ($\text{mp} = 2\text{-mercapto-pyridine}$), which is also exhibiting a copper atom ligated by two sulfurs and one hydrogen from the ligand in a $\kappa^3\text{-H,S,S}$ fashion.⁵ The ^{31}P NMR spectra show one signal at 15.6 and 16.2 ppm for **3** and **4**, respectively, also pointing toward the formation of only one species.

The molecular view of compound **4** is given in Figure 4. Selected bond lengths and angles are given in Table 3 and crystallographic data are shown in Table 6. The geometry at the copper center is tetrahedral. The metal is coordinated by the Tn ligand by two sulfur atoms as well as a hydrogen atom forming a 3-center-2-electron $\text{B-H}\cdots\text{Cu}$ interaction evidenced by a hydrogen copper distance of 1.96(3) Å. The fourth coordination site of the tetrahedron is occupied by the phosphorus

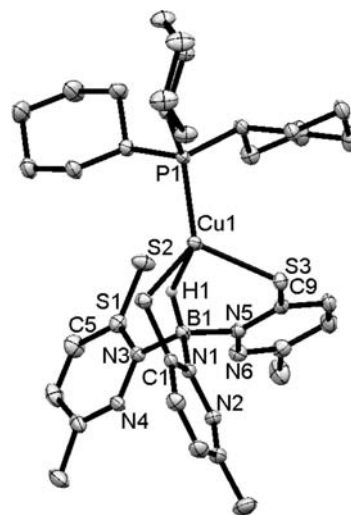


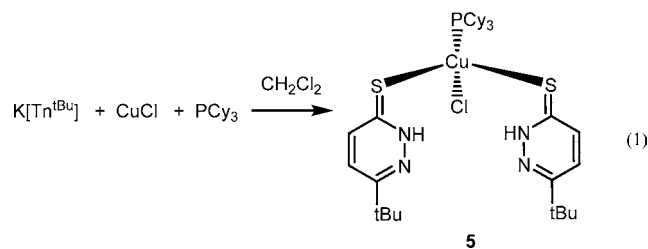
Figure 4. Molecular structure of $[\text{Cu}\{\text{Tn}^{\text{Me}}\}(\text{PCy}_3)]$ (**4**) with thermal ellipsoids at 60% probability.

Table 3. Selected Bond Lengths (Å) and Angles (deg) of $[\text{Cu}\{\text{Tn}^{\text{Me}}\}(\text{PCy}_3)]$ (**4**)

Cu1–H1J	1.96(3)	S1–Cu1–H1J	81.2(7)
Cu1–P1	2.2202(5)	S1–Cu1–P1	130.16(2)
Cu1–S1	2.2826(5)	S3–Cu1–P1	118.76(2)
Cu1–S3	2.3523(5)	P1–Cu1–H1J	114.1(7)
S1–C1	1.7091(18)	S3–Cu1–H1J	85.3(7)
B1–N1	1.566(2)	Cu1–H1J–B1	133(2)
B1–N3	1.555(2)	N3–B1–N5	111.3(1)
B1–N5	1.561(2)	N1–B1–N3	109.3(1)
S1–Cu1–S3	109.23(2)	N1–B1–N5	108.1(1)

atom of the phosphine ligand. The bonding situation at the boron center is best described as “inverted” where the hydrogen is pointing toward the metal. Interestingly, similar tripodal ligands containing Tm are usually coordinating to Cu(I) in a $\kappa^3\text{S,S,S}$ fashion exhibiting a “normal” boron center with the hydrogen pointing away from the metal,²⁴ whereas disubstituted ligands $[\text{H}_2\text{B}(\text{mim})_2]^-$ ($\text{mim} = 2\text{-mercaptoimidazolyl}$) mostly coordinate to the metal in an “inverted” $\kappa^3\text{-H,S,S}$ mode.¹⁹ The hydrogen copper distance is 1.831(2) Å in $[\text{Cu}\{\text{HBPh}(\text{mim}^{\text{Me}})_2\}(\text{PPh}_3)]$ ²⁰ and 1.832(17) Å in $[\text{Cu}\{\text{H}_2\text{B}(\text{mp})_2\}(\text{PPh}_3)]$ ⁵ which is significantly shorter compared to the here described $[\text{Cu}\{\text{Tn}^{\text{Me}}\}(\text{PCy}_3)]$ (**4**). Furthermore, H-Cu distances in borohydride ligated copper complexes like $[\text{Cu}(\text{MeC-CH}_2\text{-PPh}_2)_3(\text{HBH}_3)]$ ²¹ and $[\text{Cu}(\text{PMePh}_2)_3(\text{HBH}_3)]$ ²² are even shorter (1.605 and 1.698 Å, respectively). The bond distance between copper and the phosphorus atom is 2.2202(5) Å, being in the range of $[\text{Cu}\{\text{HBPh}(\text{mim}^{\text{Me}})_2\}(\text{PPh}_3)]$ (2.2163(8) Å) and $[\text{Cu}\{\text{B}(\text{mp})_2\}(\text{PPh}_3)]$ (2.216(3) Å). The copper sulfur distances are 2.2826(5) Å for Cu1–S1 and 2.3523(5) for Cu1–S3 which are comparable to $[\text{Cu}\{\text{HBPh}(\text{mim}^{\text{Me}})_2\}(\text{PPh}_3)]$, where Cu1–S1 is 2.2892(8) and Cu1–S2 is 2.3210(8) Å and longer compared to $[\text{Cu}\{\text{H}_2\text{B}(\text{mp})_2\}(\text{PPh}_3)]$ (2.255(4) and 2.248(4) Å for Cu1–S1 and Cu1–S2, respectively). The S1–Cu1–S3 and S1–Cu1–H1 angles of 109.23(2)° and 81.2(7)°, respectively, exhibit the distortion of the copper center. The nitrogen boron angles vary between 108.1(1)° for N1–B1–N5 and 111.3(1) for N3–B1–N5, which is exhibiting the distorted tetrahedral geometry of the boron center.

Interestingly, when reacting $K[Tn^{tBu}]$ with PCy_3 and $CuCl$ in CH_2Cl_2 instead of MeOH for 24 h, a mixture of compound **3** and the decomposition product $[Cu(Pn^{tBu})_2(PCy_3)Cl]$ (**5**) in 1:1 ratio was observed in the 1H NMR spectrum. Upon further reaction for several weeks, only compound **5** could be observed by 1H NMR spectroscopy. It was isolated as red material in pure form albeit in low yield (eq 1). As dichloromethane can



effect nondegradative reactions with sulfur-thione ligating scorpionate ligands such as Tm, giving the salt $[H_2C(mim^{Me})_2BH(mim^{Me})]Cl \cdot H_2O$ which exhibits the formation of an S-CH₂-S linkage,²³ it is conceivable that degradative reactions can take place also and that the B-N bond of Tn can be broken. This is undermined by the fact that oxidizing metal salts such as $Cu(II)Cl_2$ can cause ligand decomposition.^{6,7,20} Recrystallization from an acetonitrile solution gave crystals suitable for X-ray diffraction analysis. A molecular view is given in Figure 5. Selected bond lengths and angles are listed in Table 4 and crystallographic data are shown in Table 6. The

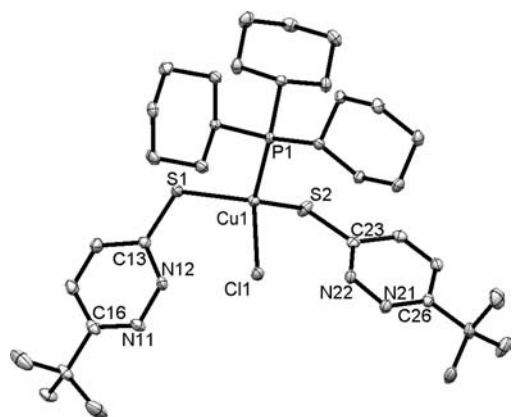


Figure 5. Molecular structure of $[Cu(Pn^{tBu})_2(PCy_3)Cl]$ (**5**) with thermal ellipsoids at 60% probability.

Table 4. Selected Bond Lengths (Å) and Angles (deg) of $[Cu(Pn^{tBu})_2(PCy_3)Cl]$ (**5**)

Cu1–Cl	2.3941(6)	Cl1–Cu1–S1	109.79(2)
Cu1–P1	2.2649(6)	Cl1–Cu1–S2	108.01(2)
Cu1–S1	2.3345(6)	S1–Cu1–P1	108.76(2)
Cu1–S2	2.3695(6)	S2–Cu1–P1	115.65(2)
S1–C13	1.690(2)	Cl1–Cu1–P1	109.52(2)
P1–C31	1.870(2)	Cu1–S1–C13	112.98(7)
P1–C41	1.860(2)	Cu1–S2–C23	109.55(7)
P1–C51	1.852(2)	Cu1–P1–C31	118.76(6)
S1–Cu1–S2	104.95(2)	Cu1–P1–C41	109.02(7)

geometry of the copper center is best described as distorted tetrahedral. The two pyridazines are binding to copper via the thione-sulfur atom and not via nitrogen, which shows the

Table 5. Electronic and Geometric Properties of $[M\{B(Pn^H)_3\}Cl]$ ($M = Cu, Ni, Co$) and $[Cu\{B(C_6H_4P(iPr)_2)_3\}Cl]$ at the B3-LYP def2-TZVP Level of Theory

	$d(M \cdots B)$ /Å	SEN ^a ($M \cdots B$)	atomic charges ^a	
			Cu	B
$[Cu\{B(Pn^H)_3\}Cl]$	2.11	0.487	0.529	−0.114
$[Ni\{B(Pn^H)_3\}Cl]$	2.05	0.672	0.589	−0.200
$[Co\{B(Pn^H)_3\}Cl]$	2.12	0.646	0.623	−0.230
$[Cu\{B(C_6H_4P(iPr)_2)_3\}Cl]$	2.57	0.398	0.466	−0.003

^aTwo center Shared Electron Number (SEN) and atomic charges with multicenter corrections as calculated by population analysis based on molecular orbitals.²⁸

higher affinity of copper to the softer sulfur atom compared to nitrogen. The copper–sulfur bond lengths are 2.3345(6) and 2.3695(6) Å for Cu1–S1 and Cu1–S2, respectively which is in the range of the copper–sulfur bonds in compound **4** and longer compared to the Cu–S distance of 2.221(2) Å in $[Cu(P(o\text{-tolyl})_3)(pymtH)Cl]$ ($pymtH = \text{pyrimidine-2-thione}$).²⁴ The Cu1–Cl bond of 2.3941(6) Å is longer than in $[Cu(P(o\text{-tolyl})_3)(pymtH)Cl]$ (2.293(2) Å) whereas the Cu1–P1 bond length is in the range of the Cu–P bond length in the other compound. The distorted tetrahedral geometry is evident by the S1–Cu1–S2 angle of 104.95(2)°, which is significantly smaller than the ideal tetrahedral angle, whereas the S1–Cu1–P1 and S2–Cu1–P1 angles are larger (108.76(2) and 115.65(2)°, respectively) but smaller than the P–Cu–S angle of 130.9(1)° in $[Cu(P(o\text{-tolyl})_3)(pymtH)Cl]$.

Theoretical Calculations. According to the Covalent Bond Classification (CBC) system the boron atom in boratrane belongs to Z type ligands forming a dative covalent bond from the metal to boron where both electrons are provided by the metal.²⁵ As a logical consequence, the d^n electron count is reduced by 2 electrons, much in the same way as the d^n count is decreased by one electron upon coordination of an X ligand (one electron from both, the metal and X). Applying this model, in the here described boratrane the d^n count is thus considered as d^8 and the boron ligand as $[BR_3]^{2-}$.^{7,26} However, a different description of the bonding situation has emerged in the literature by using the notation $(M \rightarrow B)^n$ where n refers to the number of electrons associated with the metal d orbitals; thus, $(M \rightarrow B)^{10}$ in **1**.²⁷ Nevertheless, the latter is a rarely used notation so that the information is not easily disclosed. Both notations are indicating that the bonding description of boratrane compounds by formalistic electron counting models is challenging. The short $M \rightarrow B$ interaction in our boratrane is in line with a two electron donation from the metal to boron and thus a d^8 configuration of the metal.

For a better understanding the bonding situation in the copper boratrane complex, $[Cu\{B(Pn^H)_3\}Cl]$ was investigated by DFT calculations. The hybrid density functional B3-LYP was chosen to compare the copper boratrane to similar cobalt and nickel boratrane, $[Co\{B(Pn^H)_3\}Cl]$ and $[Ni\{B(Pn^H)_3\}Cl]$, respectively (Table 5).⁶ Furthermore, calculations of shared electron numbers (SEN) were carried out for **1** as well as for Bourissou's copper boratrane complex $[Cu\{B(C_6H_4P(iPr)_2)_3\}Cl]$, the latter featuring a significantly longer $Cu \cdots B$ bond distance.¹⁵

The SENs for the pair $Cu \cdots B$ strongly indicate the presence of a copper boron bond in both copper boratrane complexes,

Table 6. Crystallographic Data and Structure Refinement for Complexes 1–5

	1	2	4	5
empirical formula	C ₂₄ H ₃₃ BClCuN ₆ S ₃ ·1.75(CH ₂ Cl ₂)	C ₄₈ H ₆₈ B ₂ Cu ₂ N ₁₂ S ₆ ·3(CH ₂ Cl ₂)	C ₃₃ H ₄₉ BCuN ₆ PS ₃ ·3(CH ₂ Cl ₂)	C ₃₄ H ₅₇ ClCuN ₄ PS ₂
<i>M_r</i> , g/mol	760.16	1408.98	986.06	715.92
cryst description	needle, orange	block, red	block, yellow	plate, red
cryst syst	monoclinic	monoclinic	triclinic	triclinic
space group	<i>P</i> 2(1)/ <i>c</i>	<i>C</i> 2/ <i>c</i>	<i>P</i> $\bar{1}$	<i>P</i> $\bar{1}$
<i>a</i> , Å	9.3659(4)	16.5494(6)	11.2357(14)	9.7963(4)
<i>b</i> , Å	22.7579(9)	17.6573(7)	12.9285(17)	9.9745(4)
<i>c</i> , Å	17.5854(7)	24.1261(9)	16.999(2)	19.2362(8)
α , deg	90	90	75.682(5)	82.217(2)
β , deg	95.193(2)	107.4795(9)	74.773(4)	81.372(2)
γ , deg	90	90	78.656(4)	85.079(2)
vol, Å ³	3732.9(3)	6724.5(4)	2285.5(5)	1837.12(13)
<i>Z</i>	4	4	2	2
<i>T</i> , K	200(2)	100(2)	100(2)	100(2)
<i>D_c</i> , g/cm ³	1.353	1.392	1.433	1.294
μ (MoK α), mm ⁻¹	1.100	1.101	1.035	0.853
<i>F</i> (000)	1566	2920	1024	764
reflns collected	78885	32372	107332	19141
unique reflns	9236	9765	12055	8828
reflns with <i>I</i> \geq 2 σ (<i>I</i>)	7170	8486	10832	6612
<i>R</i> (int)	0.0344	0.0179	0.0479	0.0381
no. of params/restraints	409/12	399/0	514/4	420/0
final <i>R</i> 1 ^a , <i>wR</i> 2 ^b (<i>I</i> \geq 2 σ)	0.0540, 0.1529	0.0298, 0.0762	0.0372, 0.0990	0.0372, 0.0784
<i>R</i> indices (all data)	0.0745, 0.1757	0.0373, 0.0811	0.0432, 0.1084	0.0614, 0.0874
GOF on <i>F</i> ²	1.087	1.023	1.085	1.006
larg. diff. peak and hole, e/Å ³	1.929, -1.010	0.693, -0.885	1.780, -1.120	0.553, -0.512
data CCDC	835862	835860	835861	835859

$${}^a R1 = \sum ||F_o| - |F_c|| / \sum |F_o|. \quad {}^b wR2 = \{ \sum [w(F_o^2 - F_c^2)^2] / \sum [w(F_o^2)^2] \}^{1/2}.$$

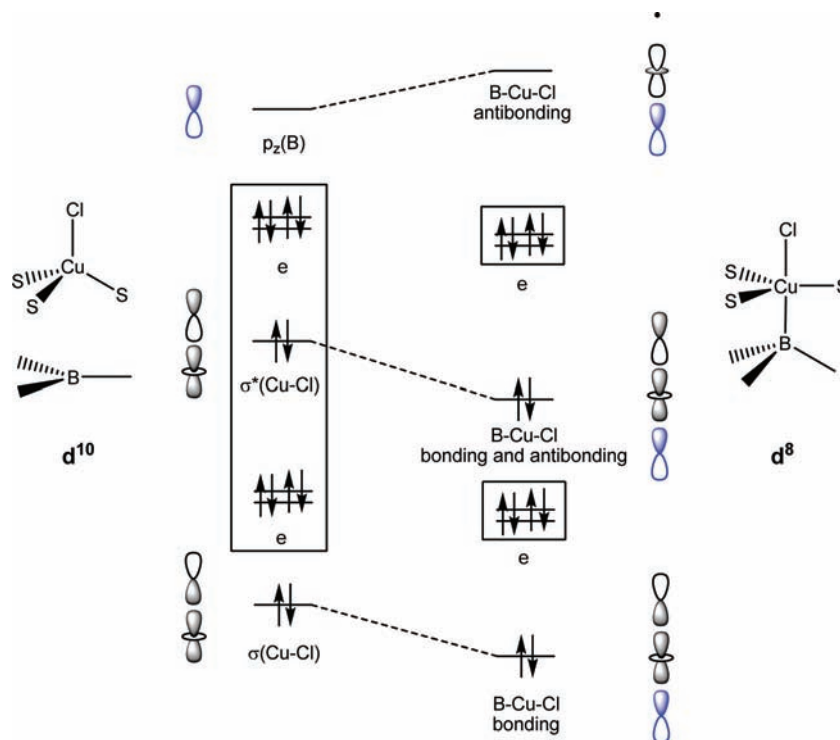


Figure 6. Orbital correlation diagram for the formation of a copper boratrane at the B3-LYP def2-TZVP level of theory.

[Cu{B(Pn^H)₃}Cl] and [Cu{B(C₆H₄P(iPr)₂)₃}Cl], respectively. The metal boron bond in Bourissou's complex, however, is much weaker compared to our system. In Bourissou's

compound less electron density is shifted from the occupied *d_z²* orbital of the metal center to the empty *p_z* orbital of the boron atom as indicated by the atomic charges derived from

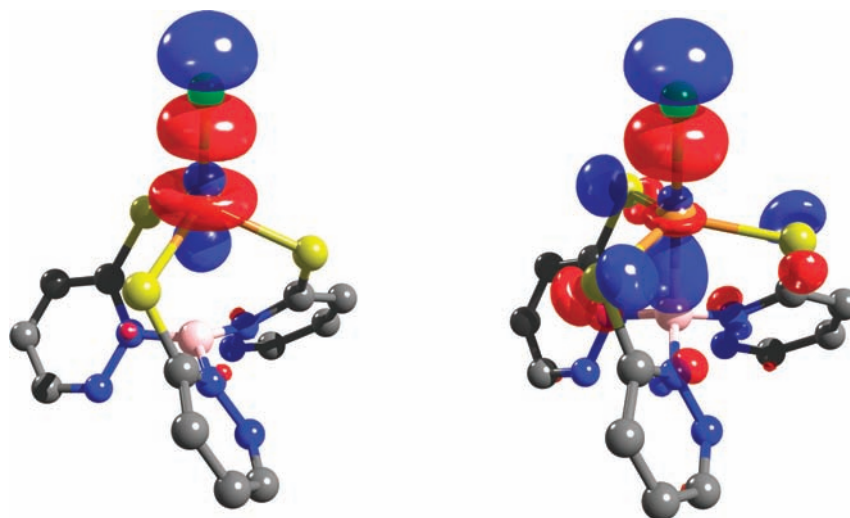


Figure 7. HOMO-2 of $[\text{Cu}\{\text{B}(\text{Pn}^{\text{H}})_3\}\text{Cl}]$ with a Cu–B distance of 3 Å (left) and of 2.11 Å (right) at the B3-LYP def2-TZVP level of theory.

population analysis. Hence, as the Cu···B bond distance increases from 2.11 Å in **1** to 2.57 Å in $[\text{Cu}\{\text{B}(\text{C}_6\text{H}_4\text{P}(\text{iPr})_2)_3\}\text{Cl}]$, the SEN decreases from 0.487 to 0.398. Although there is still a significant M→B interaction in both boratrane systems, this interaction is much stronger in the case of the nickel and cobalt boratrane complexes featuring d^7 or d^6 electron configuration, respectively.⁶ This is consistent with the concept of a metal boron bond requiring a shift of electron density from the metal to the boron atom. Generally, this M→B interaction is strengthened by electron rich metals. However, electron density shift from a fully occupied d^{10} metal center leading to a d^8 copper boratrane system is energetically less favorable.

DFT calculations support a d^8 configuration for the copper boratrane complex $[\text{Cu}\{\text{B}(\text{Pn}^{\text{H}})_3\}\text{Cl}]$. In a hypothetical d^{10} system featuring a Cu–B distance of 3 Å all 10 d electrons can be assigned to the metal as the p_z orbital on the planar boron atom remains unoccupied (Figure 6). Upon formation of the copper boratrane bond, electron density is shifted from the bonding and antibonding σ -orbitals describing the Cu–Cl bond toward the boron atom thus leading to a 4-electron-3-center B–Cu–Cl interaction. It is best represented by a bonding orbital B–Cu–Cl, a mixed bonding and antibonding B–Cu–Cl orbital, and an unoccupied antibonding B–Cu–Cl orbital, respectively. The remaining 8 d-electrons are metal based and thus leading to a d^8 configuration. Furthermore, formation of the copper boratrane significantly affects the geometry altering the metal environment from tetrahedral to trigonal bipyramidal. The shift of electron density from the metal to the boron atom is represented by the HOMO-2 of $[\text{Cu}\{\text{B}(\text{Pn}^{\text{H}})_3\}\text{Cl}]$ (Figure 7). In comparison, Bourissou's copper boratrane complex with a significantly longer Cu–B bond has a weaker interaction and thus was described by the authors as having a d^{10} configuration.

CONCLUSION

We have prepared new copper complexes containing the Tn moiety. Reaction of $\text{K}[\text{Tn}^{\text{tBu}}]$ with CuCl_2 in dichloromethane gave the copper boratrane complex $[\text{Cu}\{\text{B}(\text{Pn}^{\text{tBu}})_3\}\text{Cl}]$ under activation of the B–H bond, resulting in a Cu→B dative bond. In contrast to this, reaction of $\text{K}[\text{Tn}^{\text{tBu}}]$ with CuCl in THF gave the dimeric compound $[\text{Cu}\{\text{Tn}^{\text{tBu}}\}]_2$, and addition of CuCl to a solution of PCy_3 and $\text{K}[\text{Tn}^{\text{R}}]$ (R = Me, tBu) in MeOH gave

complexes $[\text{Cu}\{\text{Tn}^{\text{R}}\}(\text{PCy}_3)]$. $[\text{Cu}\{\text{Tn}^{\text{tBu}}\}]_2$ and $[\text{Cu}\{\text{Tn}^{\text{R}}\}(\text{PCy}_3)]$ exhibit a 3-center-2-electron B–H···Cu interaction, as evidenced by X-ray crystallography. The nature of the M→B interaction featured in our copper boratrane compound **1** as well as in Bourissou's complex $[\text{Cu}\{\text{B}(\text{C}_6\text{H}_4\text{P}(\text{iPr})_2)_3\}\text{Cl}]$ was further investigated by DFT studies and compared to similar late transition metal systems of type $[\text{M}\{\text{B}(\text{Pn}^{\text{H}})_3\}\text{Cl}]$ (M = Co, Ni). As electron density is shifted from the electron rich boron center toward the boron atom upon formation of boratrane compounds, such M→B interactions are naturally weaker when going from an electronically fully occupied d^{10} to a d^8 system. Notably, our copper boratrane features a stronger metal boron bond than Bourissou's system as evidenced by calculation of shared electron numbers (SEN) as well as by X-ray crystallography.

EXPERIMENTAL SECTION

General Procedures. NMR spectra were measured on a Bruker Avance III 300 MHz spectrometer. ^1H NMR and ^{13}C NMR spectroscopy chemical shift values are reported as δ using the solvent signal ($\text{DMSO}-d_6$: δ 2.50 and 39.4 or 7.26 and 77.0 ppm for $\text{DMSO}-d_6$ or CDCl_3 , respectively) as an internal standard. Spectra were obtained at 25 °C. Mass spectra were measured on an Agilent LCMSSD single quadrupole mass spectrometer of the SL type. The mass spectrometer was equipped with an atmospheric pressure ionization (API) source employing pneumatically assisted electrospray nebulization with nitrogen as the nebulizer gas. Elemental analyses were performed on a Heraeus VARIO ELEMENTAR by the Analytisch-Chemisches Laboratorium des Instituts für Anorganische Chemie der Technischen Universität Graz, Austria. Infrared spectra were recorded on a Perkin-Elmer FT-IR spectrometer 1725X as KBr pellets and on a Bruker Alpha Platinum ATR spectrometer.

Ligands $\text{K}[\text{Tn}^{\text{tBu}}]$ and $\text{K}[\text{Tn}^{\text{Me}}]$ were synthesized according to published procedures.⁶

X-ray Structure Determinations. For X-ray structure analyses for all compounds the crystals were mounted onto the tip of glass fibers and covered in inert oil. Data collection was performed on a BRUKER-AXS SMART APEX II CCD diffractometer using graphite-monochromated Mo $K\alpha$ radiation (0.71073 Å) at 100(2) K (except **1** at 200(2) K). The data for all compounds were reduced to F^2_o and corrected for L_p with SAINT.²⁹ Absorption correction was performed with SADABS.³⁰ The structures were solved by direct methods³¹ using the WinGX suite of programs³² and refined by full-matrix least-squares method with SHELXS-97.³³ If not noted otherwise all non-hydrogen atoms were refined with anisotropic displacement parameters. All

hydrogen atoms were fixed in calculated positions to correspond to standard bond lengths and angles, apart from the hydridic hydrogens, which were located in the difference map and allowed to refine isotropically.

Computational Details. The geometry of $[\text{Cu}\{\text{B}(\text{Pn}^{\text{H}})_3\}\text{Cl}]$ was optimized in the gas phase using the hybrid density functional B3LYP³⁴ as implemented in the TURBOMOLE³⁵ program. First geometry optimization was performed with the standard double- ζ quality basis def2-SVP.³⁶ The geometry was then reoptimized with the larger def2-TZVP basis.^{36b,37} Input geometry of $[\text{Cu}\{\text{B}(\text{Pn}^{\text{H}})_3\}\text{Cl}]$ was obtained from the crystal structure of $[\text{Cu}\{\text{B}(\text{Pn}^{\text{tBu}})_3\}\text{Cl}]$ (1) by removing the bulky *tert*-butyl groups at the pyridazine moiety. The stationary point was confirmed as minimum by calculation of analytical harmonic frequencies. Natural population analysis (NPA)³⁸ as well as calculations of the shared electron number (SEN)³⁹ were performed with the larger def2-TZVP basis. The shared electron number gives the number of electrons shared by bonded atoms which cannot be assigned to either atom in a unique way. The shared electron numbers can be considered as a measure of covalent bond strength.²⁸ For reason of comparison, calculations of SENs were also performed on Bourissou's boratrane system $[\text{Cu}\{\text{B}(\text{C}_6\text{H}_4\text{P}(\text{iPr})_2)_3\}\text{Cl}]$ using their optimized geometry.¹⁵ The geometry of $[\text{Cu}\{\text{B}(\text{Pn}^{\text{H}})_3\}\text{Cl}]$ with a weak Cu–B interaction was optimized with a constrained Cu–B distance of 3 Å with the def2-TZVP basis. Molecular orbitals were visualized with Avogadro.³⁵

$[\text{Cu}\{\text{B}(\text{Pn}^{\text{tBu}})_3\}\text{Cl}]$ (1). A stirred solution of $\text{K}[\text{Tn}^{\text{tBu}}]$ (0.30 g, 0.54 mmol) in CH_2Cl_2 (10 mL) was treated with $\text{CuCl}_2 \cdot 2\text{H}_2\text{O}$ (0.093 g, 0.54 mmol). After 15 h the orange suspension was filtrated, washed with 3 mL of CHCl_3 , 6 mL of H_2O , 2 mL of MeOH, and 3 mL of Et_2O . The thus obtained orange solid was dried in vacuo giving 118 mg (36%) of 1. Crystals suitable for X-ray diffraction analysis were obtained by recrystallization from a dichloromethane solution. ¹H NMR (DMSO-*d*₆, 300 MHz) δ 1.07 (s, 3H, C(CH₃)₃), 7.97 (d, 1H, ³J_{H–H} = 9.29 Hz, HS), 8.09 (d, 1H, ³J_{H–H} = 9.28 Hz, H4) ppm. ¹³C NMR (DMSO-*d*₆, 75 MHz) δ 28.2 (C(CH₃)₃), 36.2 (C(CH₃)₃), 129.1 (C5), 136.1 (C4), 162.7 (C6), 176.3 (C=S) ppm. MS (ESI) *m/z* = 575.2 (38%) [M – Cl]⁺. IR (ATR, cm^{–1}): 1592 m, 1477 m, 1428 s, 1256 s, 649 s, 588 s. Anal. Calcd for C₂₄H₃₃N₆BClCuS₃·0.56CH₂Cl₂: C, 44.76; H, 5.22; N, 12.75%. Found: C, 44.76; H, 5.06; N, 12.97%.

$[\text{Cu}\{\text{HB}(\text{Pn}^{\text{tBu}})_3\}]_2$ (2). Method 1: A stirred solution of $\text{K}[\text{Tn}^{\text{tBu}}]$ (0.30 g, 0.54 mmol) in THF (35 mL) was treated with CuCl (0.054 g, 0.54 mmol) giving a red solution. After 24 h of stirring the solvent was removed in vacuo. Recrystallization from a dichloromethane solution gave red crystals. They were isolated by filtration giving 0.25 g (75%) of 2.

Method 2: A stirred solution of $\text{K}[\text{HB}(\text{Pn}^{\text{tBu}})_3]$ (0.20 g, 0.36 mmol) in H₂O (25 mL) was treated with $\text{CuCl}_2 \cdot 2\text{H}_2\text{O}$ (0.061 g, 0.36 mmol) resulting in immediate formation of a red precipitate. The suspension was stirred for 15 min, and the product was isolated by filtration and dried in vacuo for 24 h giving 0.126 g (30%) of 2. Crystals suitable for X-ray diffraction analysis were obtained by recrystallization from a dichloromethane/diethyl ether solution (1:8 v/v). ¹H NMR (CDCl₃, 300 MHz) δ 1.05 (s, 34H, C(CH₃)₃), 7.06 (d, 6H, pyridazine-H5, J_{H–H} = 9.1 Hz), 7.83 (d, 6H, pyridazine-H4, J_{H–H} = 9.1 Hz). ¹³C NMR (CDCl₃, 75 MHz) δ 29.00 (C(CH₃)₃), 36.3 (C(CH₃)₃), 122.1 (C5), 140.8 (C4), 160.2 (C6), 177.6 (C=S) ppm. MS (ESI) *m/z* = 807.2 (100%) [M – {B(Pn^{tBu})₂}]⁺. IR (KBr pellets, cm^{–1}), 2963 m, 1477 s, 1430 s, 1210 m, 1144 s, 834 w. Anal. Calcd for C₄₈H₆₈B₂Cu₂N₁₂S₆·0.75 H₂O: C, 48.08; H, 5.75; N, 13.80%. Found: C, 48.08; H, 5.31; N, 13.80%.

$[\text{Cu}\{\text{HB}(\text{Pn}^{\text{tBu}})_3\}(\text{PCy}_3)]$ (3). Tricyclohexyl phosphine (0.304 g, 1.08 mmol) was added to a stirred solution of $\text{K}[\text{Tn}^{\text{Me}}]$ (0.300 g, 0.54 mmol) in MeOH (18 mL). After addition of CuCl (0.054 g, 0.54 mmol) an orange suspension was formed which was stirred for 29 h. The orange reaction product was collected by filtration, washed with 5 mL of MeOH and dried in vacuo, giving 264 mg (57%) of yellow product 3. ¹H NMR (CDCl₃, 300 MHz) δ 1.04 (s, 27H, C(CH₃)₃), 1.22–1.89 (m, 37H, Cy-H), 6.96 (d, 3H, pyridazine-H5, J_{H–H} = 9.13 Hz), 7.70 (d, 3H, pyridazine-H4, J_{H–H} = 9.11 Hz) ppm. ¹³C NMR (CDCl₃, 75 MHz) δ 26.3 (Cy-C), 27.5 (Cy-C), 28.9 (C(CH₃)₃), 30.3

(Cy-C), 31.9 (Cy-C), 36.2 (C(CH₃)₃), 121.3 (C5), 140.4 (C4), 159.0 (C6), 178.7 (C=S) ppm. ³¹P NMR (CDCl₃, 121 MHz) δ 15.6 ppm. MS (ESI) *m/z* = 689.2 (59%) [M – Pn^{tBu}]⁺. IR (ATR, cm^{–1}): 2922 s, 1476 m, 1426 s, 1177 s, 852 s. Anal. Calcd for C₄₂H₆₇BCuN₆PS₃: C, 58.82; H, 7.88; N, 9.80%. Found: C, 58.12; H, 7.69; N, 9.67%.

$[\text{Cu}\{\text{HB}(\text{Pn}^{\text{Me}})_3\}(\text{PCy}_3)]$ (4). Tricyclohexyl phosphine (0.203 g, 0.72 mmol) was added to a stirred suspension of CuCl (0.036 g, 0.36 mmol) in MeOH (10 mL). After addition of $\text{K}[\text{Tn}^{\text{Me}}]$ (0.154 g, 0.36 mmol) the suspension was stirred for 3 days. The dark yellow reaction mixture was filtered, and the obtained solid was dissolved in CH₂Cl₂. After filtration the solvent was removed in vacuo. Recrystallization from a dichloromethane solution gave orange crystals. They were isolated by filtration and washed with 5 mL of MeOH giving 75 mg (21%) of 4. Crystals suitable for X-ray diffraction analysis were obtained by recrystallization from a dichloromethane solution. ¹H NMR (CDCl₃, 300 MHz) δ 1.91–1.18 (m, 30H, Cy-H), 2.23 (s, 9H, CH₃), 5.89 (br s, 1H, B-H), 6.76 (d, 3H, ³J_{H–H} = 8.90 Hz, HS), 7.67 (d, 3H, ³J_{H–H} = 8.87 Hz, H4). ¹³C NMR (CDCl₃, 75 MHz) δ 21.7 (CH₃), 26.3 (Cy-C), 27.4 (Cy-C), 27.5 (Cy-C), 30.3 (Cy-C), 30.3 (Cy-C), 31.8 (Cy-C), 31.9 (Cy-C), 124.8 (C5), 140.6 (C4), 150.0 (C6), 178.8 (C=S) ppm. ³¹P NMR (CDCl₃, 121 MHz) δ 16.2 ppm. MS (ESI) *m/z* = 607.2 (12%) [M – Pn^{tBu}]⁺. IR (ATR, cm^{–1}): 2921 s, 1428 s, 1216 s, 1103 s, 888 m. Anal. Calcd for C₃₃H₄₉BCuN₆PS₃: C, 54.20; H, 6.75; N, 11.49%. Found: C, 54.18; H, 6.83; N, 11.42%.

$[\text{Cu}(\text{Pn}^{\text{tBu}})_2(\text{PCy}_3)\text{Cl}]$ (5). Tricyclohexyl phosphine (0.203 g, 0.72 mmol) was added to a stirred suspension of CuCl (0.036 g, 0.36 mmol) in degassed abs. CH₂Cl₂ (10 mL). After addition of $\text{K}[\text{Tn}^{\text{tBu}}]$ (0.154 g, 0.36 mmol) the suspension was stirred for 26 days. The red reaction mixture was filtered, and the solvent was removed in vacuo. Recrystallization from an acetonitrile solution gave red crystals. They were isolated by filtration giving 47 mg (18%) of 5. Crystals suitable for X-ray diffraction analysis were obtained by recrystallization from an acetonitrile solution.

¹H NMR (CDCl₃, 300 MHz) δ 1.28 (s, 18H, C(CH₃)₃), 1.93–1.33 (m, 34 H, Cy-H), 7.22 (d, 2H, pyridazine-H5, J_{H–H} = 9.35 Hz), 7.63 (d, 2H, pyridazine-H4, J_{H–H} = 9.34 Hz), 14.43 (s, 2H, NH) ppm. ¹³C NMR (CDCl₃, 75 MHz) δ 26.2 (Cy-C), 27.5 (Cy-C), 28.7 (C(CH₃)₃), 30.39 (Cy-C), 32.0 (Cy-C), 36.5 (C(CH₃)₃), 125.6 (C5), 139.8 (C4), 162.0 (C6), 175.2 (C=S) ppm. ³¹P NMR (CDCl₃, 121 MHz) δ 9.9 ppm. IR (ATR, cm^{–1}): 2963 m, 1476 m, 1428 s, 1255 s, 926 s, 649 s; Anal. Calcd for C₃₄H₅₇ClCuN₄PS₂: C, 57.04; H, 8.02; N, 8.96%. Found: C, 56.65; H, 8.07; N, 8.25%.

■ ASSOCIATED CONTENT

📄 Supporting Information

Crystallographic data in CIF format. This material is available free of charge via the Internet at <http://pubs.acs.org>.

■ AUTHOR INFORMATION

Corresponding Author

*E-mail: nadia.moesch@uni-graz.at.

■ REFERENCES

- (1) (a) Trofimenko, S. *Scorpionates: The Coordination Chemistry of Polypyrazolylborate Ligands*; Imperial College Press: London, 1999. (b) Pettinari, C. *Scorpionates II: Chelating Borate Ligands*; Imperial College Press: London, 2008. (c) Tolman, W. J. *Biol. Inorg. Chem.* **2006**, *11*, 261–271. (d) Kitajima, N.; Moro-oka, Y. *Chem. Rev.* **1994**, *94*, 737–757.
- (2) Trofimenko, S. *J. Am. Chem. Soc.* **1966**, *88*, 1842–1844.
- (3) Garner, M.; Reglinski, J.; Cassidy, I.; Spicer, M. D.; Kennedy, A. R. *Chem. Commun.* **1996**, 1975–1976.
- (4) Ge, P.; Haggerty, B. S.; Rheingold, A. L.; Riordan, C. G. *J. Am. Chem. Soc.* **1994**, *116*, 8406–8407.
- (5) Dyson, G.; Hamilton, A.; Mitchell, B.; Owen, G. R. *Dalton Trans.* **2009**, 6120–6126.
- (6) Nuss, G.; Saischek, G.; Harum, B. N.; Volpe, M.; Gatterer, K.; Belaj, F.; Möscher-Zanetti, N. C. *Inorg. Chem.* **2011**, *50*, 1991–2001.

- (7) Spicer, M. D.; Reglinski, J. *Eur. J. Inorg. Chem.* **2009**, 2009, 1553–1574.
- (8) Garner, M.; Lewinski, K.; Pattek-Janczyk, A.; Reglinski, J.; Sieklucka, B.; Spicer, M. D.; Szaleniec, M. *Dalton Trans.* **2003**, 1181–1185.
- (9) Jesson, J. P.; Trofimenko, S.; Eaton, D. R. *J. Am. Chem. Soc.* **1967**, 89, 3158–3164.
- (10) Iwata, S.; Ostermeier, C.; Ludwig, B.; Michel, H. *Nature* **1995**, 376, 660–669.
- (11) Ibrahim, M. M.; Shaban, S. Y. *Inorg. Chim. Acta* **2009**, 362, 1471–1477.
- (12) (a) Patel, D. V.; Mihalcik, D. J.; Kreisel, K. A.; Yap, G. P. A.; Zakharov, L. N.; Kassel, W. S.; Rheingold, A. L.; Rabinovich, D. *Dalton Trans.* **2005**, 2410–2416. (b) Bailey, P. J.; Dawson, A.; McCormack, C.; Moggach, S. A.; Oswald, I. D. H.; Parsons, S.; Rankin, D. W. H.; Turner, A. *Inorg. Chem.* **2005**, 44, 8884–8898. (c) Gioia Lobbia, G.; Pettinari, C.; Santini, C.; Somers, N.; Skelton, B. W.; White, A. H. *Inorg. Chim. Acta* **2001**, 319, 15–22.
- (13) (a) Hill, A. F.; Owen, G. R.; White, A. J. P.; Williams, D. J. *Angew. Chem., Int. Ed.* **1999**, 38, 2759–2761. (b) Foreman, M. R. S. J.; Hill, A. F.; White, A. J. P.; Williams, D. J. *Organometallics* **2004**, 23, 913–916. (c) Crossley, I. R.; Foreman, M. R. S. J.; Hill, A. F.; White, A. J. P.; Williams, D. J. *Chem. Commun.* **2005**, 221–223. (d) Crossley, I. R.; Hill, A. F. *Organometallics* **2004**, 23, 5656–5658. (e) Mihalcik, D. J.; White, J. L.; Tanski, J. M.; Zakharov, L. N.; Yap, G. P. A.; Incarvito, C. D.; Rheingold, A. L.; Rabinovich, D. *Dalton Trans.* **2004**, 1626–1634. (f) Crossley, I. R.; Hill, A. F.; Willis, A. C. *Organometallics* **2005**, 24, 1062–1064. (g) Figueroa, J. S.; Melnick, J. G.; Parkin, G. *Inorg. Chem.* **2006**, 45, 7056–7058. (h) Senda, S.; Ohki, Y.; Hirayama, T.; Toda, D.; Chen, J.-L.; Matsumoto, T.; Kawaguchi, H.; Tatsumi, K. *Inorg. Chem.* **2006**, 45, 9914–9925. (i) Pang, K.; Quan, S. M.; Parkin, G. *Chem. Commun.* **2006**, 5015–5017.
- (14) Sircoglou, M.; Bontemps, S.; Mercy, M.; Miqueu, K.; Ladeira, S.; Saffon, N.; Maron, L.; Bouhadir, G.; Bourissou, D. *Inorg. Chem.* **2010**, 49, 3983–3990.
- (15) Sircoglou, M.; Bontemps, S.; Fontaine, F.-G.; Boudreau, J.; Thibault, M.-H.; Bourissou, D. *J. Am. Chem. Soc.* **2008**, 130, 16729–16729.
- (16) Carrier, S. M.; Ruggiero, C. E.; Houser, R. P.; Tolman, W. B. *Inorg. Chem.* **1993**, 32, 4889–4899.
- (17) Cammi, R.; Gennari, M.; Giannetto, M.; Lanfranchi, M.; Marchio, L.; Mori, G.; Paiola, C.; Pellinghelli, M. A. *Inorg. Chem.* **2005**, 44, 4333–4345.
- (18) Careri, M.; Elviri, L.; Lanfranchi, M.; Marchiò, L.; Mora, C.; Pellinghelli, M. A. *Inorg. Chem.* **2003**, 42, 2109–2114.
- (19) (a) Kimblin, C.; Bridgewater, B. M.; Hascall, T.; Parkin, G. *Dalton Trans.* **2000**, 891–897. (b) Videira, M.; Moura, C.; Datta, A.; Paulo, A. n.; Santos, I. C.; Santos, I. *Inorg. Chem.* **2009**, 48, 4251–4257. (c) Alvarez, H. M.; Krawiec, M.; Donovan-Merkert, B. T.; Fouzi, M.; Rabinovich, D. *Inorg. Chem.* **2001**, 40, 5736–5737.
- (20) Dodds, C. a.; Garner, M.; Reglinski, J.; Spicer, M. D. *Inorg. Chem.* **2006**, 45, 2733–2741.
- (21) Ghilardi, C. A.; Midollini, S.; Orlandini, A. *Inorg. Chem.* **1982**, 21, 4096–4098.
- (22) Takusagawa, F.; Fumagalli, A.; Koetzle, T. F.; Shore, S. G.; Schmitkons, T.; Fratini, A. V.; Morse, K. W.; Wei, C.-Y.; Bau, R. *J. Am. Chem. Soc.* **1981**, 103, 5165–5171.
- (23) Crossley, I. R.; Hill, A. F.; Humphrey, E. R.; Smith, M. K.; Tshabang, N.; Willis, A. C. *Chem. Commun.* **2004**, 1878–1879.
- (24) Hadjikakou, S. K.; Aslanidis, P.; Karagiannidis, P.; Aubry, A.; Skoulika, S. *Inorg. Chim. Acta* **1992**, 193, 129–135.
- (25) Green, M. L. H. *J. Organomet. Chem.* **1995**, 500, 127–148.
- (26) (a) Parkin, G. *Organometallics* **2006**, 25, 4744–4747. (b) Landry, V. K.; Melnick, J. G.; Buccella, D.; Pang, K.; Ulichny, J. C.; Parkin, G. *Inorg. Chem.* **2006**, 45, 2588–2597. (c) Blagg, R. J.; Charmant, J. P. H.; Connelly, N. G.; Haddow, M. F.; Orpen, A. G. *Chem. Commun.* **2006**, 2350–2352.
- (27) Hill, A. F. *Organometallics* **2006**, 25, 4741–4743.
- (28) Zirz, C.; Ahlrichs, R. *Inorg. Chem.* **1984**, 23, 26–31.
- (29) SAINTPLUS, Software Reference Manual, version 6. 4; Bruker AXS: Madison, WI, 1997.
- (30) (a) SADABS, version 2.1; Bruker AXS: Madison, WI, 1998. (b) Blessing, R. H. *Acta Crystallogr., Sect. A: Found. Crystallogr.* **1995**, 51, 33–38.
- (31) Sheldrick, G. M. *SHELXS-97*; University of Göttingen: Göttingen, Germany, 1997.
- (32) Farrugia, L. J. *J. Appl. Crystallogr.* **1999**, 32, 837–838.
- (33) Sheldrick, G. M. *Acta Crystallogr., Sect. A: Found. Crystallogr.* **2008**, 64, 112–122.
- (34) (a) Becke, A. D. *J. Chem. Phys.* **1993**, 98, 1372–1377. (b) Lee, C.; Yang, W.; Parr, R. G. *Phys. Rev. B* **1988**, 37, 785–789.
- (35) Rainka, M. P.; Milne, J. E.; Buchwald, S. L. *Angew. Chem.* **2005**, 117, 6333–6336.
- (36) (a) Schäfer, A.; Horn, H.; Ahlrichs, R. *J. Chem. Phys.* **1992**, 97, 2571. (b) Weigend, F.; Ahlrichs, R. *Phys. Chem. Chem. Phys.* **2005**, 7, 3297–3305.
- (37) Weigend, F.; Häslers, M.; Patzelt, H.; Ahlrichs, R. *Chem. Phys. Lett.* **1998**, 294, 143–152.
- (38) Reed, A. E.; Weinstock, R. B.; Weinhold, F. *J. Chem. Phys.* **1985**, 83, 735–746.
- (39) Ehrhardt, C.; Ahlrichs, R. *Theor. Chim. Acta* **1985**, 68, 231–245.